

Fig. 2 Velocity profiles at a change in injection rate.

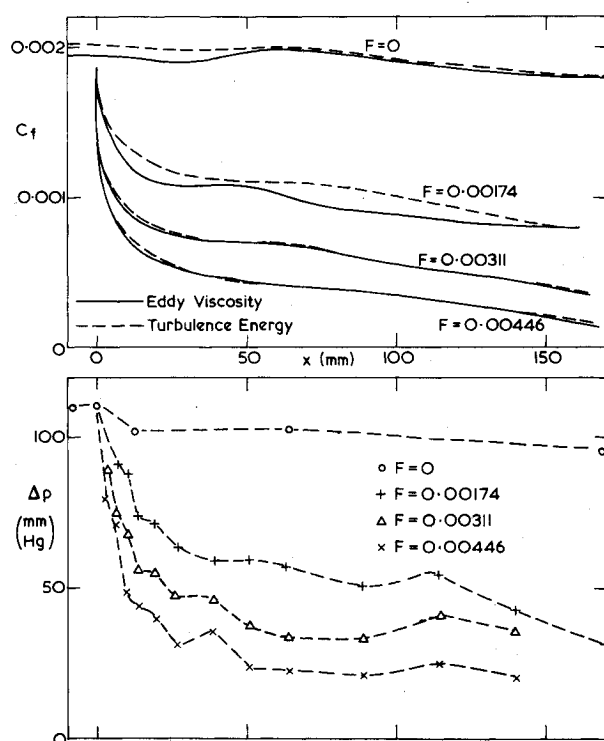


Fig. 3 Skin-friction results: solid to porous surface.

perature is assumed to be related to the velocity by the Crocco relation, i.e.

$$\frac{T}{T_1} = \frac{T_w}{T_1} + \left(\frac{T_r}{T_1} - \frac{T_w}{T_1} \right) \frac{u}{U_1} + \left(1 - \frac{T_r}{T_1} \right) \left(\frac{u}{U_1} \right)^2$$

Here $T_r = T_1 (1 + [(\gamma - 1)/2] r M_1^2)$, with $r = 0.89$ for solid surfaces. There is very little experimental data for the value of the recovery factor r for porous surfaces, but based on these limited data the formula $r = 0.89(1 + 1.66F/c_f)^{-0.04}$ was used in the present calculations. All the measured temperatures

were compared with the Crocco relation and with the temperatures predicted by the eddy viscosity model which does solve the energy equation. Except for the adverse pressure gradient with high injection rates the experimental results were in fair agreement with the predictions of the eddy viscosity model and with the Crocco relation. In general the predictions of the eddy viscosity model and the Crocco relation differ by less than 3° (i.e., by less than 1% of stagnation temperature) throughout the layer. Since the estimated error of the measured temperature can be up to 3° , it is impossible to differentiate between the two prediction methods.

Conclusions

From the preceding discussion it is clear that both prediction methods are satisfactory for the prediction of flows with combined injection and favorable pressure gradient, and for the initial development of the flow over a blown surface. However, neither method is completely satisfactory for flow with combined injection and adverse pressure gradient, or for the re-establishment of the flow downstream of a region of injection.

It would appear that for all the flows considered here the use of the Crocco relation is just as accurate as, and far more convenient than, the solution of the energy equation.

References

- Jeromin, L. O. F., "An Experimental Investigation of the Compressible Turbulent Boundary Layer with Air Injection," R&M 3526, British Aeronautical Research Council, 1968.
- Squire, L. C., "Further Experimental Investigations of Compressible Turbulent Boundary Layers with Air Injection," R&M 3627, British Aeronautical Research Council, 1970.
- Dunbar, D. I. A. and Squire, L. C., "Experiments in Turbulent Boundary Layers with Foreign Gas Injection," R&M 3696, British Aeronautical Research Council, 1972.
- Thomas, G. D., "Compressible Turbulent Boundary Layers with Combined Air Injection and Pressure Gradient," R&M 3779, British Aeronautical Research Council, 1976.
- Marriott, P. G., "Compressible Turbulent Boundary Layers with Discontinuous Air Transpiration," R&M 3780, British Aeronautical Research Council, 1976.
- Squire, L. C. and Verma, V. K., "The Calculation of Compressible Turbulent Boundary Layers with Air Injection," Current Paper No. 1265, British Aeronautical Research Council, 1973.
- Cebeci, T. and Smith, A. M. O., *Analysis of Turbulent Boundary Layers*, Academic Press, New York, 1974.
- Bradshaw, P. and Ferriss, D. H., "Calculation of Boundary Layer Development Using the Turbulence Energy Equation: Compressible Flow on Adiabatic Wall," *Journal of Fluid Mechanics*, Vol. 46, 1971, pp. 83-110.
- Thomas, G. D., Verma, V. K., and Squire, L. C., "A Comparison of Two Prediction Methods with Experiment for Compressible Turbulent Boundary Layers with Air Injection," *Aeronautical Quarterly*, Vol. XXIII, 1972, pp. 301-306.
- Smith, K. G., Gaudet, L., and Winter, K. G., "The Use of Surface Pitot Tubes as Skin-Friction Meters at Supersonic Speeds," R&M, 3351, British Aeronautical Research Council, 1964.

Transition in a Streamwise Corner

O. O. Mojola*

University of Ife, Ile-Ife, Nigeria

Nomenclature

- U = streamwise mean velocity
 X = streamwise coordinate along the corner
 H = velocity profile shape parameter

Received Aug. 5, 1976; revision received Nov. 12, 1976.

Index category: Boundary-Layer Stability and Transition.

*Lecturer, Dept. of Agricultural Engineering.

- δ = boundary-layer thickness (defined by $U = 0.995 U_\infty$)
 δ^* = displacement thickness
 θ = momentum thickness
 r = radial distance from the corner along the corner bisector
 ν = kinematic viscosity of the fluid

Subscripts

- s = corner-bisecting plane
 ∞ = freestream

Introduction

LAMINAR or turbulent flows directed parallel or roughly parallel to a streamwise corner have long aroused immense interest because of their common occurrence, as in wing-body junctions of aircraft. But our current knowledge^{1,2} of them is still rather rudimentary.

The purpose of this Note is to draw attention to some aspects of natural and artificial transition from fully laminar to fully turbulent flow in a right-angled streamwise corner (Fig. 1), formed by the intersection of two smooth flat plates with unswept leading and trailing edges, and at low subsonic speeds. All the measurements we are about to discuss were carried out in a low-speed, closed-circuit wind tunnel with a nominal freestream turbulence of 0.03%. Details of the other main facilities (corner model, traverse gear, etc.) and the measurement techniques may be found in Refs. 1 and 3.

Natural Transition

In agreement with Nomura⁴ and Zamir and Young,⁵ but in disagreement with Gersten⁶ and Perkins,⁷ transition to turbulent flow was found to occur earlier at the corner line than elsewhere on the plates. With a freestream velocity of about 30 m/sec, turbulent bursts appeared first at the corner at about 150 mm from the corner leading edge, corresponding to $U_\infty x/\nu \approx 3 \times 10^5$, which is only a little higher than the value of 2×10^5 reported by Zamir and Young,⁵ based on measurements at a lower speed ($U_\infty = 427$ cm/sec) but possibly higher freestream turbulence.

Transition from laminar to fully turbulent flow, whether natural or artificial, never occurs at a point but always stretches over a finite distance. The transitional development of streamwise mean velocity profiles in the corner bisecting plane is displayed in Fig. 2. It is noteworthy that the profile at $x = 0.15$ m, which essentially marks the end of initial laminar flow regime (and hence the beginning of the transition region), is distinctly of the "separation" type, comprehensively reported by Zamir and Young⁵ for laminar profiles along the right-angled corner bisector. The transitional profiles also show a remarkable region of nearly constant velocity (i.e., low shear) within the inner 10 to 25% of the local boundary-layer thickness from the corner. But these low shear zones shrink as the transition to fully turbulent flow progresses. The transitional profiles of Zamir and Young also exhibit some nearly constant velocity zones, but these low shear zones lie near the middle of their boundary layer. It is possible that this difference in the location of the low shear zones is due to the difference in unit Reynolds number, but this is by no means certain.

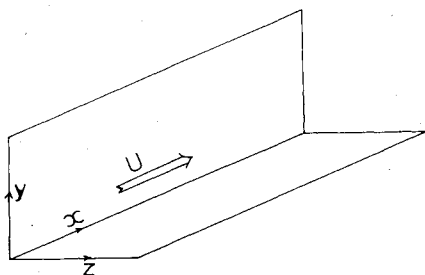


Fig. 1 The corner-flow geometry.

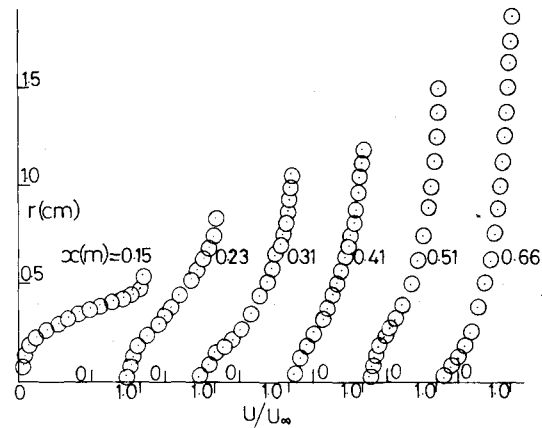


Fig. 2 Development of velocity profiles along the corner bisector with natural transition.

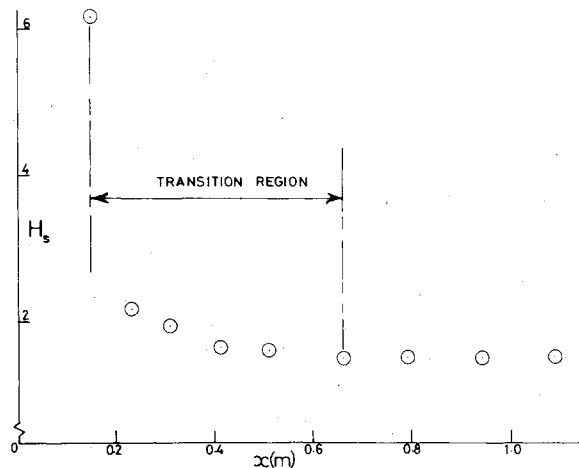


Fig. 3 Distribution of profile shape factor for 90° corner in zero pressure gradient.

To define more precisely the (hitherto loosely defined) transition region of the present experiments, one may define for the mean flow in the corner bisecting plane (because of its quasi-two-dimensionality¹), a conventional profile shape factor

$$H_s = \delta_s^* / \theta_s \quad (1)$$

where

$$\delta_s^* = \int_0^\infty \left(1 - \frac{U}{U_\infty}\right) dr, \quad \theta_s = \int_0^\infty \frac{U}{U_\infty} \left(1 - \frac{U}{U_\infty}\right) dr$$

Then the distribution of H_s for the profiles of Fig. 2 is as shown in Fig. 3, from which it may be deduced that the transition region Δx extends over $0.15 \text{ m} < x < 0.66 \text{ m}$, since $H_s \approx \text{constant} \approx 1.5$ for $x > 0.66 \text{ m}$. Shown, for comparison, in Fig. 4 is the experimental distribution of shape factor for a transitional two-dimensional flow on a flat plate (in a zero pressure gradient and 0.03% freestream turbulence), based on the measurements of Schubauer and Klebanoff⁸. If Δx denotes the extent of a transition region, then for the corner flow $\Delta x U_\infty / \nu = 1.06 \times 10^6$, which is remarkably close to $\Delta x U_\infty / \nu \approx 1.0 \times 10^6$, corresponding to the data of Schubauer and Klebanoff⁸ for the flat-plate flow. One then can appreciate that, although transition may occur relatively prematurely at a sharp corner, its subsequent development takes place at roughly the same rate as that of two-dimensional flow on a flat plate.

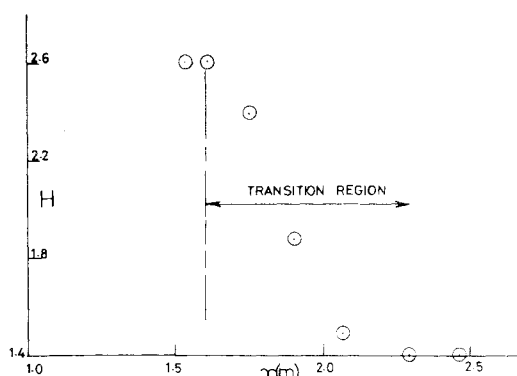


Fig. 4 Distribution of profile shape factor for two-dimensional flat-plate flow (after Schubauer and Klebanoff⁸).

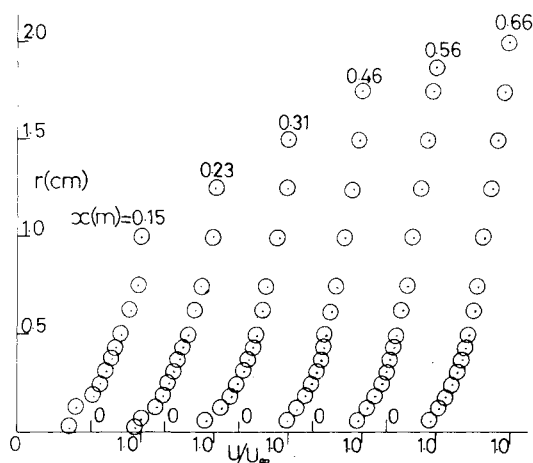


Fig. 5 Development of velocity profiles along the corner bisector with artificial transition.

Artificial Transition

An attempt was made by the present author to examine some aspects of corner flow sensitivity to artificial transition—provoking devices of different mean roughness heights. On the recommendation of Klebanoff and Diehl,⁹ who had made a thorough study of tripping devices in two-dimensional flow, sandpaper-type roughness was chosen for the investigation.

With a sandpaper roughness 25.4-mm wide and 0.75-mm high and with its upstream edge 25.4-mm downstream of the corner leading edge, the mean velocity profiles immediately downstream of the transition trip showed, in Fig. 5, some distortion. Fortunately, however, for lack of a sustaining mechanism, the distortion died out fairly quickly in the downstream direction, leaving behind at least some thickening of the boundary layer. Although the tendency toward a “self-preserving” turbulent corner flow was rapid, it was not as rapid as with natural transition. Moreover, the self-preserving form obtained with artificial transition need not be identical with that for natural transition. As a matter of fact, the shape factor H_s [defined by Eq. (1)] of the velocity profile at $x = 1.091$ m with the 0.75-mm transition trip is 1.6, which is about 7% higher than the value 1.5 (Fig. 3), corresponding to the case of natural transition.

References

- ¹Mojola, O.O., “Turbulent Boundary Layer Along a Streamwise Corner,” Ph.D. thesis, 1972, University of London, London, England.
- ²Zamir, M., “Boundary-Layer Flow in a Streamwise Corner,” Ph.D. thesis, 1968, University of London, London, England.
- ³Mojola, O.O. and Young, A.D., “An Experimental Investigation of the Turbulent Boundary Layer Along a Streamwise Corner,”

Proceedings, AGARD Conference on Turbulent Shear Flows, Sept. 1971, Paper No. 12, London.

⁴Nomura, Y., “Theoretical and Experimental Investigations of the Incompressible Viscous Flow around the Corner,” *Memoirs of the Defence Academy of Japan*, Vol. 2, No. 3, 1962.

⁵Zamir, M. and Young, A.D., “Experimental Investigation of the Boundary Layer in a Streamwise Corner,” *The Aeronautical Quarterly*, Vol. XXI, Nov. 1970, pp. 313-339.

⁶Gersten, K., “Corner Interference Effects,” AGARD Rept. 299, 1959.

⁷Perkins, H.J., “The Turbulent Corner Boundary Layer,” Ph.D. thesis, 1970, University of Cambridge, Cambridge, England.

⁸Schubauer, G.B. and Klebanoff, P.S., “Contributions on the Mechanics of Boundary-Layer Transition,” NACA TN3489, 1955; also NACA Rept. 1289, 1956.

⁹Klebanoff, P.S. and Diehl, Z.W., “Some Features of Artificially Thickened Fully Developed Turbulent Boundary Layers with Zero Pressure Gradient,” NACA Rept. 1110, 1952.

High-Potential Clouds in Jet-Engine Exhausts

J. F. Shaeffer* and T. C. Peng*

McDonnell Douglas Corporation, St. Louis, Mo.

Introduction

EXPERIMENTAL investigations conducted by the Air Force Flight Dynamics Laboratory (AFFDL) have shown that electrostatic probes placed in a jet-engine exhaust to measure ion concentrations produce unusual signal pulses (spikes). In some tests, the occurrence of pulses increased by orders of magnitude prior to failure of a gas-path engine component. Initial hopes were that this phenomenon could be utilized to indicate imminent engine failure. However, the mechanism responsible for spike production must be determined, and the relationship to gas-path component failure must be understood. This Note deals with an investigation of potential mechanisms responsible for producing the probe spike signals.

Analyses of AFFDL data and our experiments lead to the conclusion that the observed spikes are a form of negative corona (electrical discharge) known as Trichel pulses. Furthermore, probe data indicate that this negative corona is induced by positively charged, high-potential eddies or clouds which flow past the probe.

The jet-engine related experimental work was conducted by AFFDL and three industrial contractors.^{1,2†} The Electrostatic probes used in these studies were 6.3-mm diam, 7.6 to 12.7-cm-long stainless-steel cylinders with well rounded tips. The probes were electrically connected to ground (engine case) through a low-impedance, current-measuring shunt.

A typical single pulse is shown in Fig. 1a. The rise time was comparable to the response time of the instrumentation used (2-4 ns). The decay time was 0.7 μ s in this case, but varied between 0.2 and 5 μ s. The peak amplitude also varied widely, from 10 mV to several volts, corresponding to peak currents of 100 nA to tens of milliamperes. The total charge (i.e., the time integral of the current) ranged from 0.1 to 10 nC. Pulse polarity was positive, corresponding to positive ions arriving at the probe from the gas or to electrons leaving the probe and

Received July 12, 1976; presented as Paper 76-397 at the AIAA 9th Fluid and Plasma Dynamics Conference, San Diego, Calif., July 14-16, 1976; revision received Nov. 22, 1976.

Index categories: Plasma Dynamics and MHD; Combustion in Gases; Atomic, Molecular, and Plasma Properties.

*Scientist, McDonnell Douglas Research Laboratories. Member AIAA.

†References 1 and 2 contain a complete list of citations.